

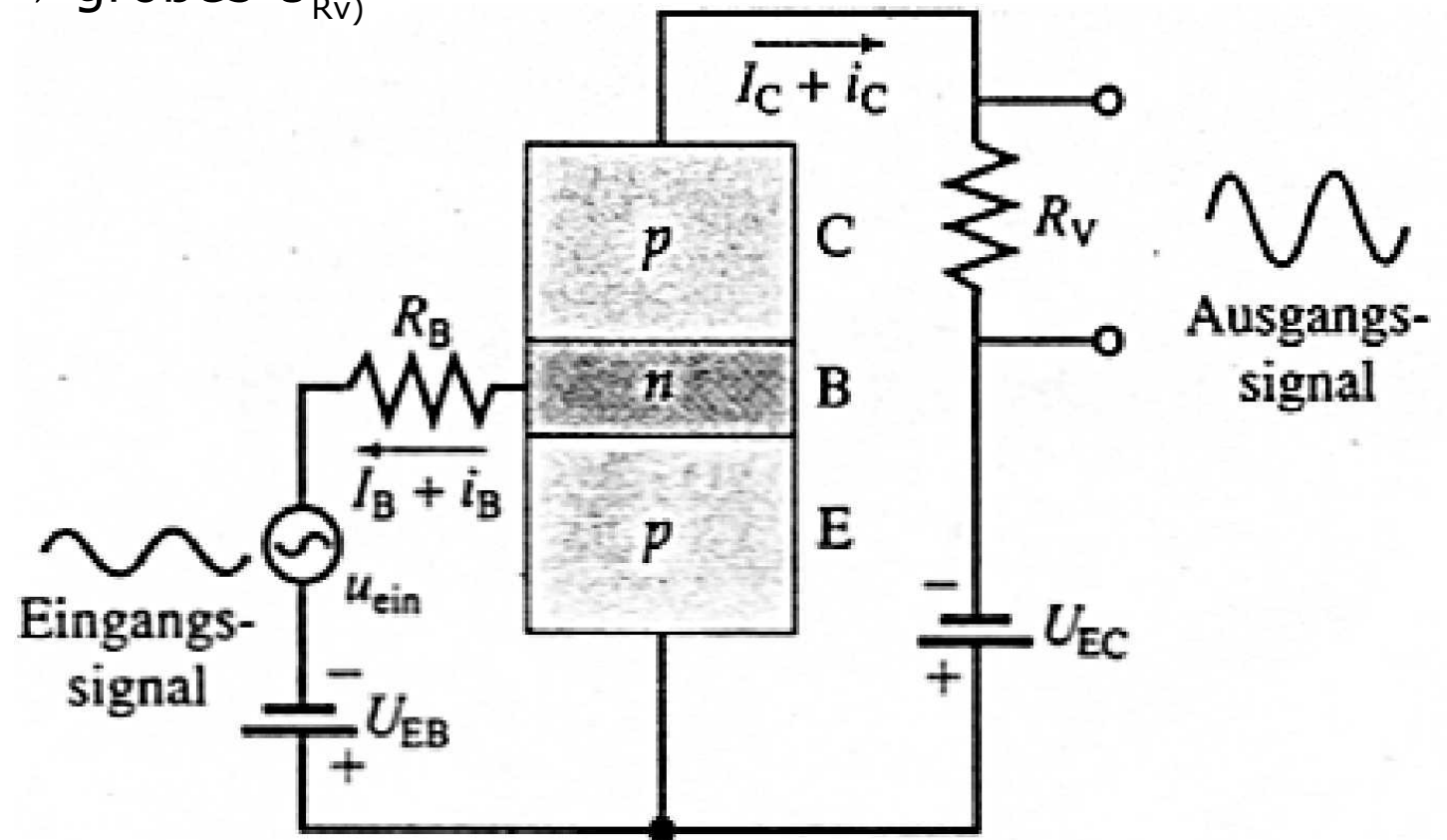
John Bardeen**, William B. Shockley und Walter Brattain (v.l.n.r., 1956)
erfanden den bipolaren Transistor 1947 in den Bell Laboratories
Originalversuchsaufbau (Quelle: Lucent Technologies)

pnp-Transistorverstärkerschaltung

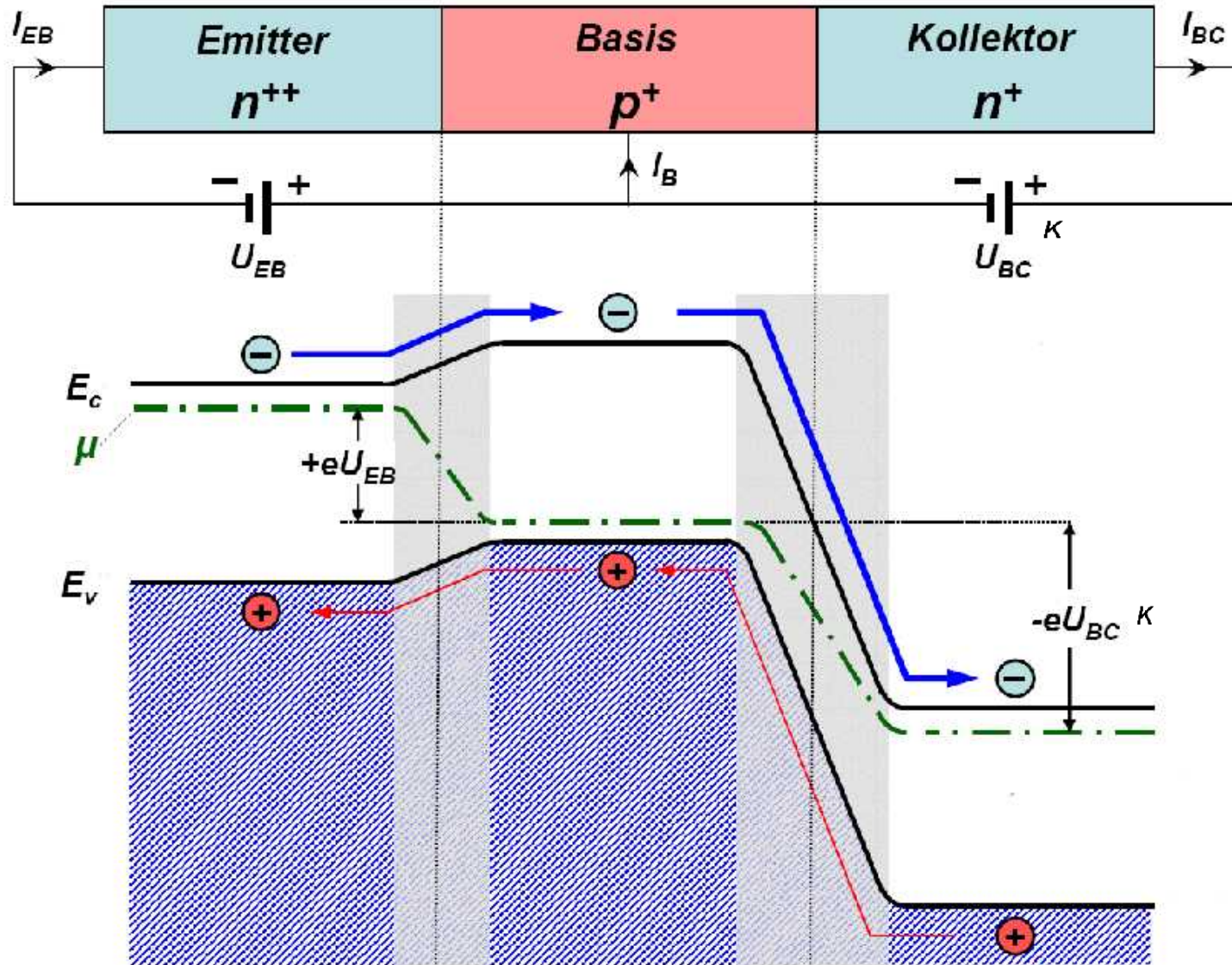
kleine Änderung i_B des Basisstroms I_B

→ große Änderung i_C des Kollektorstroms I_C

(oder: kleines u_{ein} → großes U_{Rv})



nnp-Transistor



EB in Durchlass-, BK in Sperrrichtung; Basis dünn gegen Diffusionslänge; über EB injizierte Ladungsträger diffundieren (transistor!) zu K; dort durch Sperrspannung abgesaugt

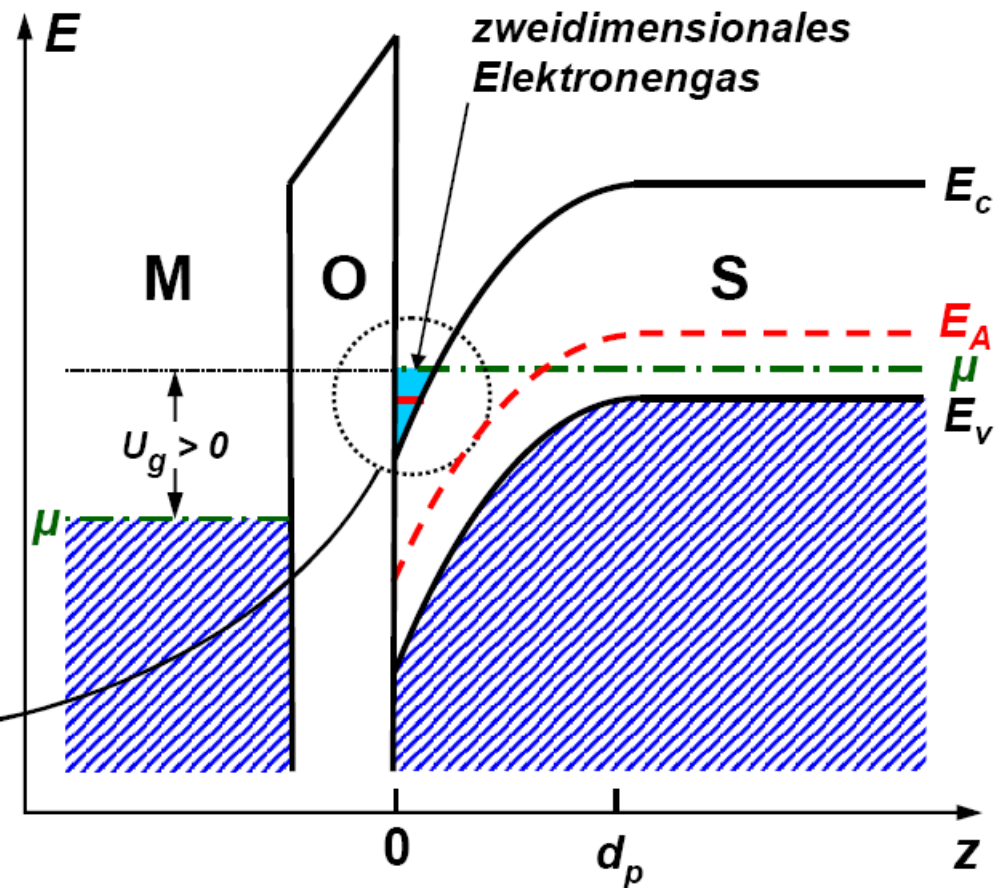
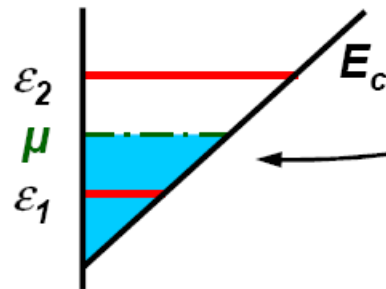
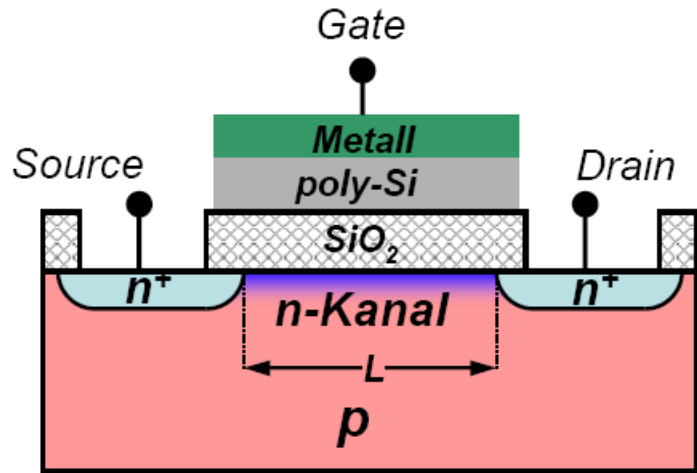
n.b.: dicke Basis hat Strom 0 zur Folge

MOSFET

Metal-Oxide-Semiconductor Field Effect Transistor (1960)

Julius E. Lilienfeld, U.S. Patent 1, 745, 175 (1930)

Oskar Heil, British Patent 439, 457 (1935)



MOSFET Gate-Spannung $U_{\text{gate}} > 0$

Gate-Feld hält Elektronen im Kanal

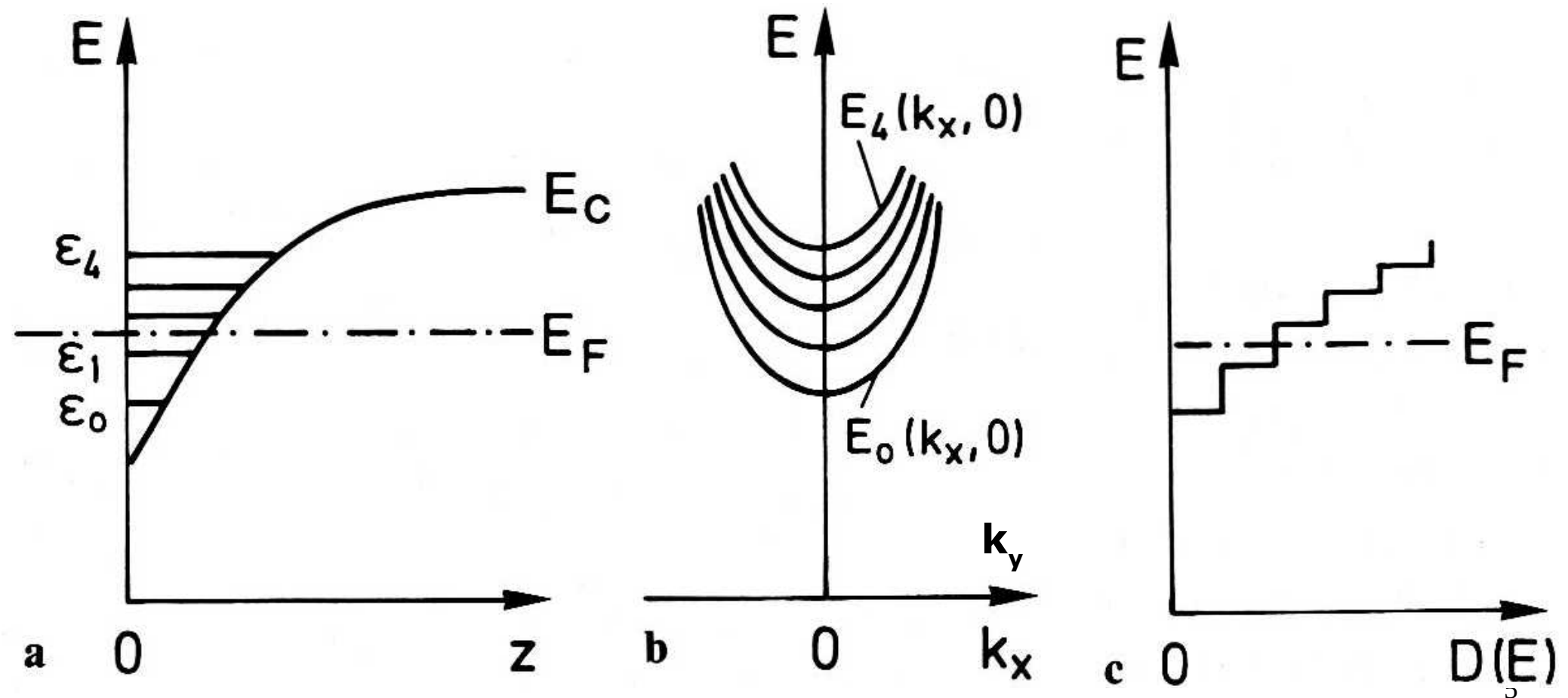
Dreieckspotenzial an Grenzfläche p -Halbleiter/Oxidschicht: 2DEG

hier unterstes Subband besetzt

"Nebeneffekt":

Niedrigdimensionale Elektronensysteme

Quantentrog (quantum well)



Andere Realisierung: Heterostrukturen

Binäre Verbindungen: GaAs 2- oder Mehrlagensysteme

Ternäre Verbindungen: $\text{Al}_x\text{Ga}_{1-x}\text{As}$

Quaternäre Verbindungen: $\text{Ga}_x\text{In}_{1-x}\text{As}_y\text{P}_{1-y}$

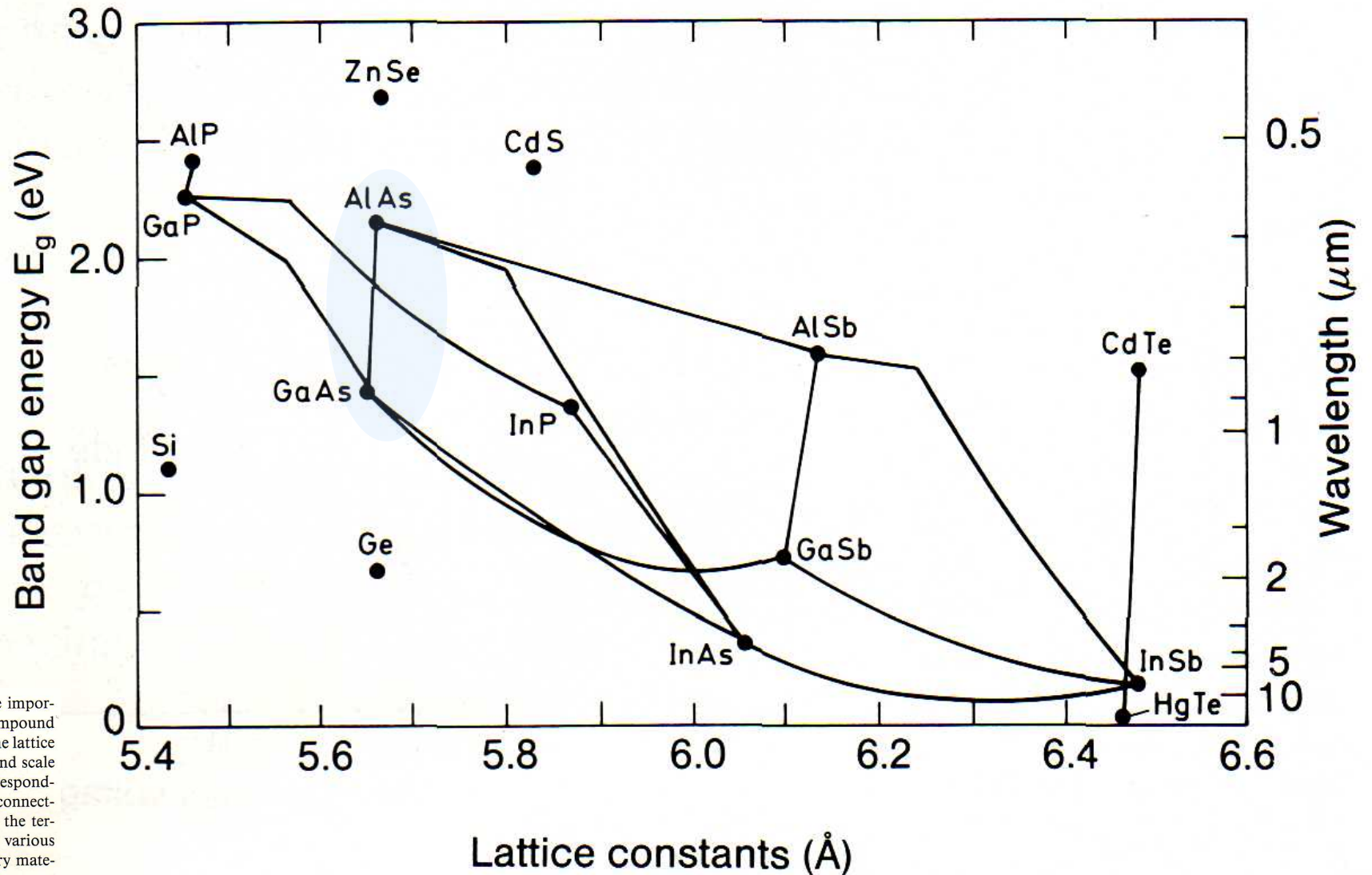
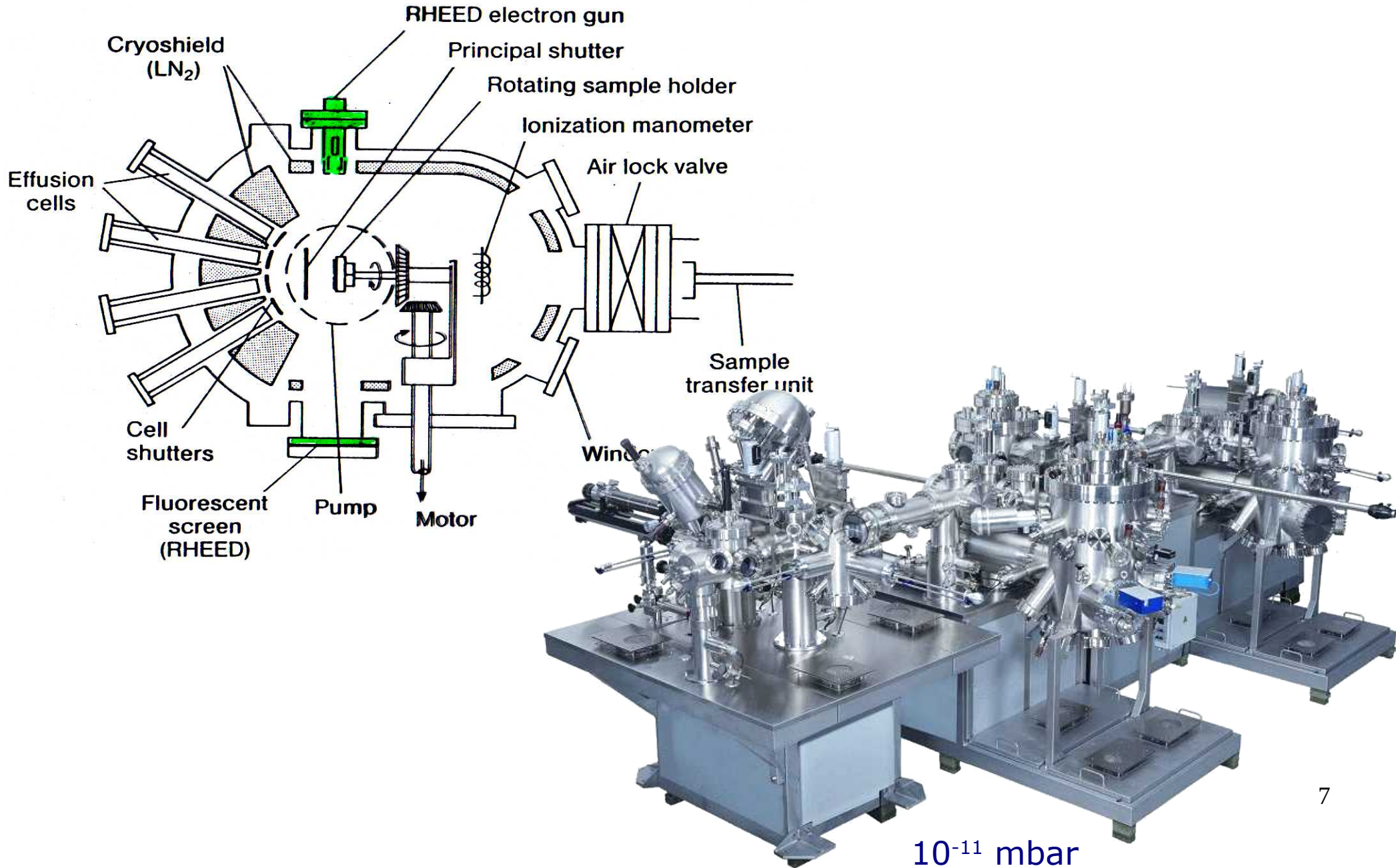


Fig. 12.21. Band gap E_g of some important elemental and binary compound semiconductors plotted against the lattice parameter at 300 K. The right-hand scale gives the light wavelength λ corresponding to the band gap energy. The connecting lines give the energy gaps of the ternary compounds composed of various ratios of the corresponding binary materials

Molekularstrahlepitaxie (MBE)

Metal Organic Chemical Vapour Deposition (MOCVD)



10⁻¹¹ mbar

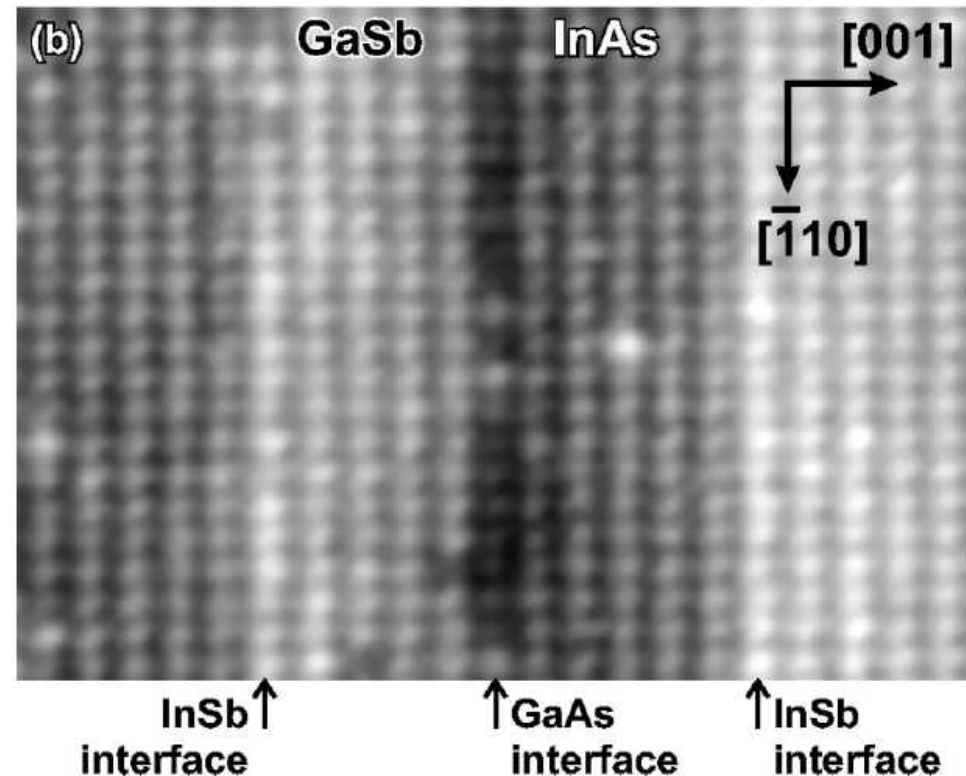
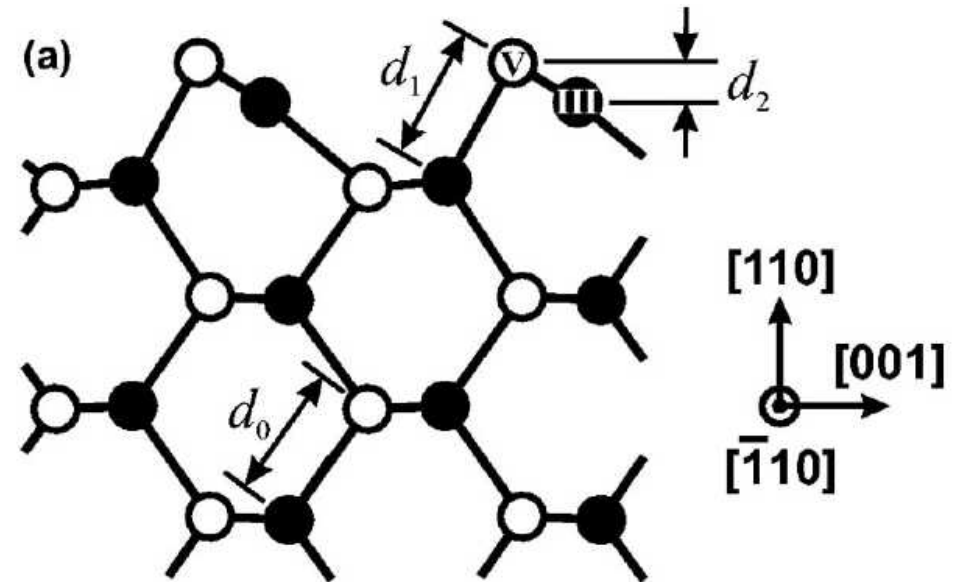
Ausdehnung der Übergangszone ?

Strukturell: 1 Atomlage

Elektronisch:

Bandlücke 1 Atomlage

Bandverbiegung λ_D (≈ 10 nm)



PHYSICAL REVIEW B 67, R121306 (2003)

(a) Relaxed geometry of a III-V (110) surface.

d_0 : bond length in the bulk

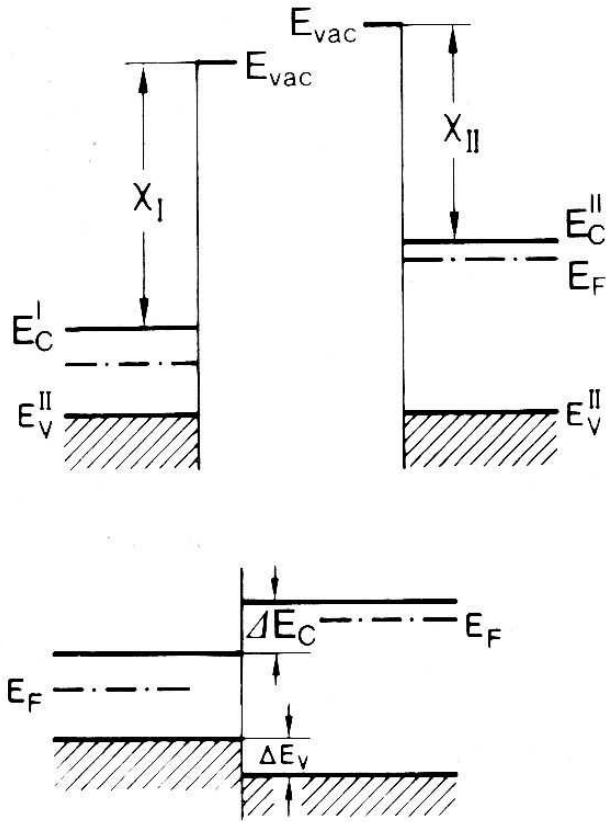
d_1 : surface III-V bond length indicated

d_2 : III-V height difference at surface

(b) Constant-current, filled-state STM image of

InAs/GaAs superlattice

Semiconductor I Semiconductor II



Im Gleichgewicht:

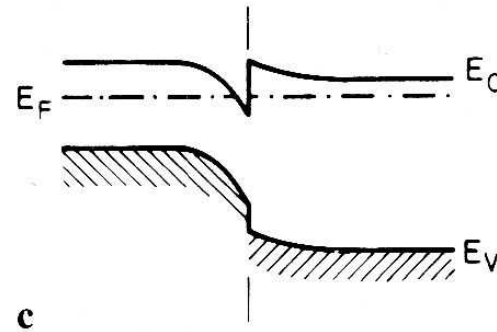


Fig. 12.22 a–c. Band schemes (one-electron energies plotted in real space) for a heterostructure formed from semiconductors I and II. **a** Semiconductors I and II are assumed to be isolated; χ_I and χ_{II} are the electron affinities, i.e., the energy between the vacuum energy E_{vac} and the lower conduction band edge E_C . **b** Semiconductors I and II are in contact, but not in thermal equilibrium because the Fermi levels E_F on the two sides have not equalized. ΔE_C and ΔE_V are the band discontinuities in the conduction and valence bands, respectively. **c** In thermal equilibrium, the Fermi energies E_F in I and II must be identical. Since the band discontinuities ΔE_C and ΔE_V are predetermined, band bending must occur in the two semiconductors

χ Elektronenaffinität

Leitungsbanddiskontinuität $\Delta E_C = \chi_1 - \chi_2$

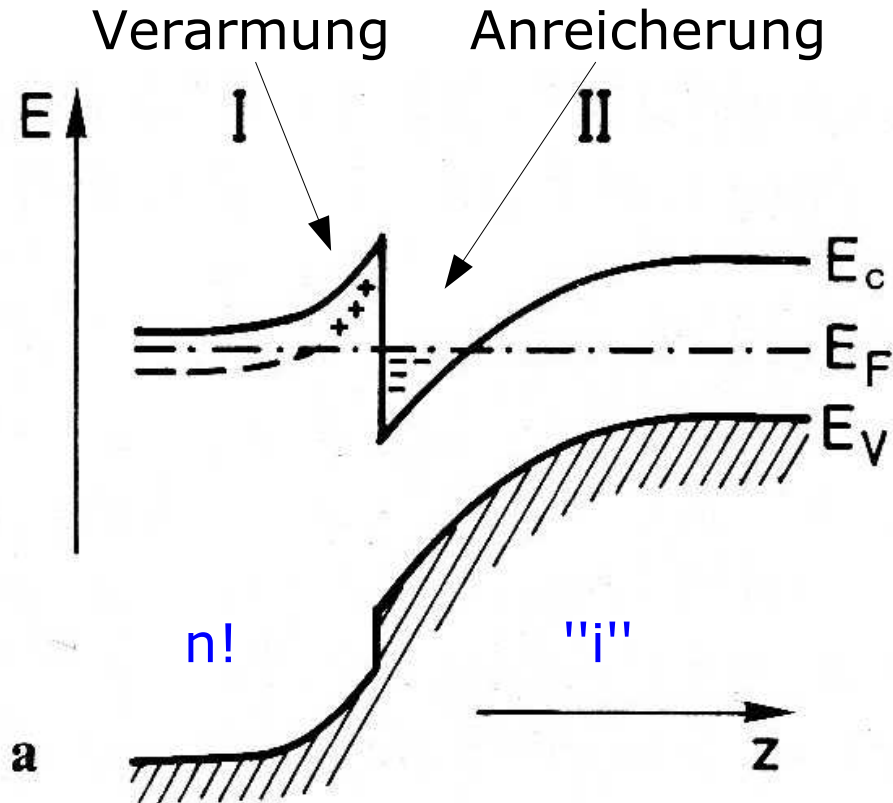
(Obacht: Oberflächendipol, Defekt/Grenzflächenzustände)

Modulation doping

N-n heterojunction

I: wide gap heavily n-doped

II: narrower gap weakly n-doped



Electrons confined against AlGaAs by E-field of dopants (Si^+)

band scheme of superlattice

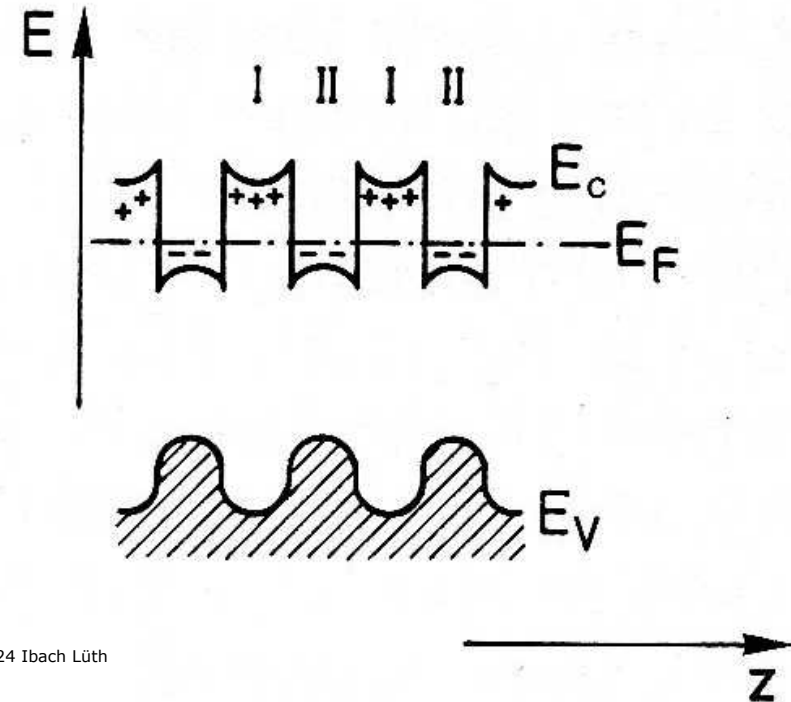
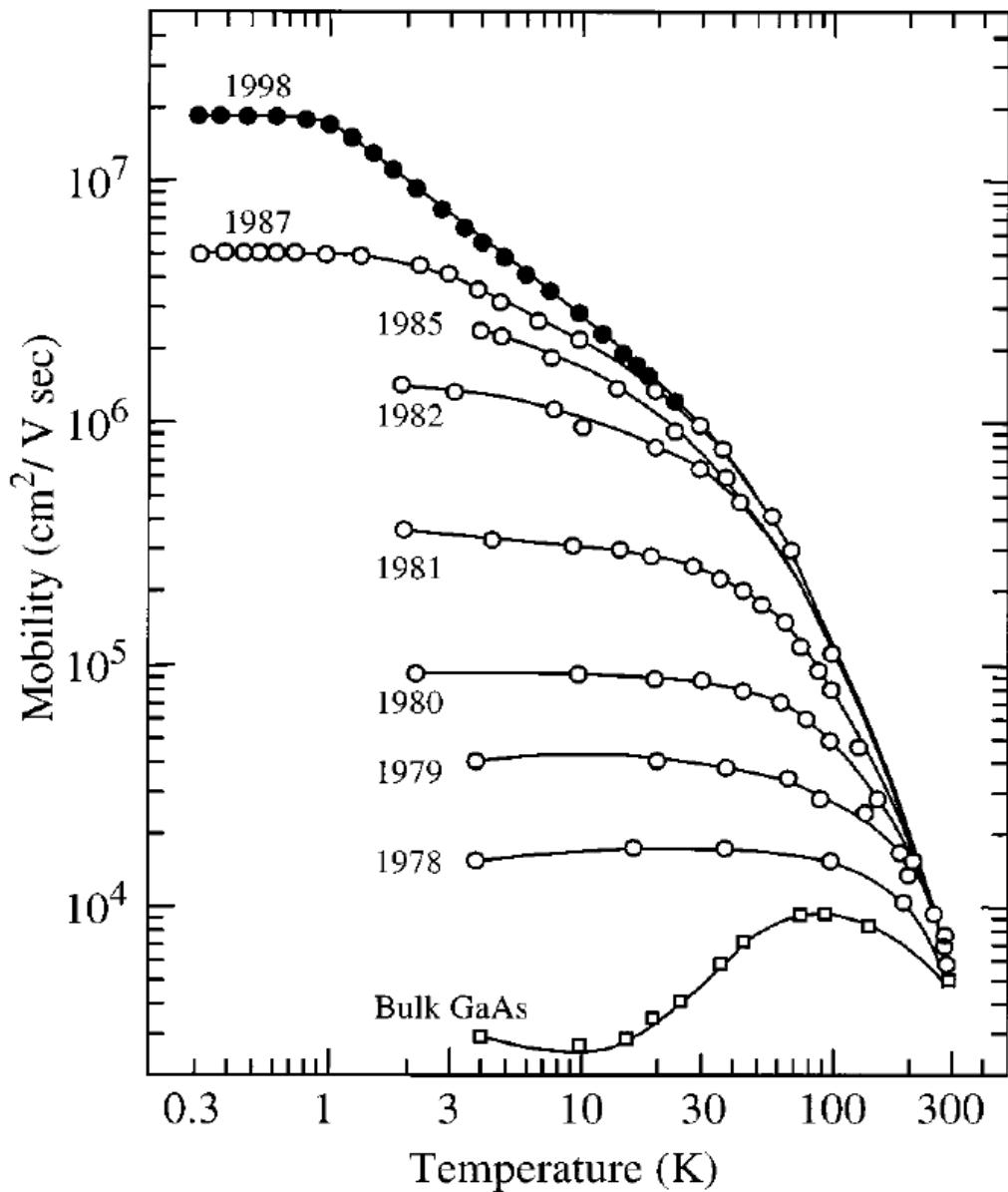


Fig. 12.24 Ibach Lüth

Electron mobility of 2DEGs in modulation doped GaAs/AlGaAs



high T / lowest T: μ limited by scattering from phonons / defects

Progress made: Thousandfold increase of μ through modulation doping.

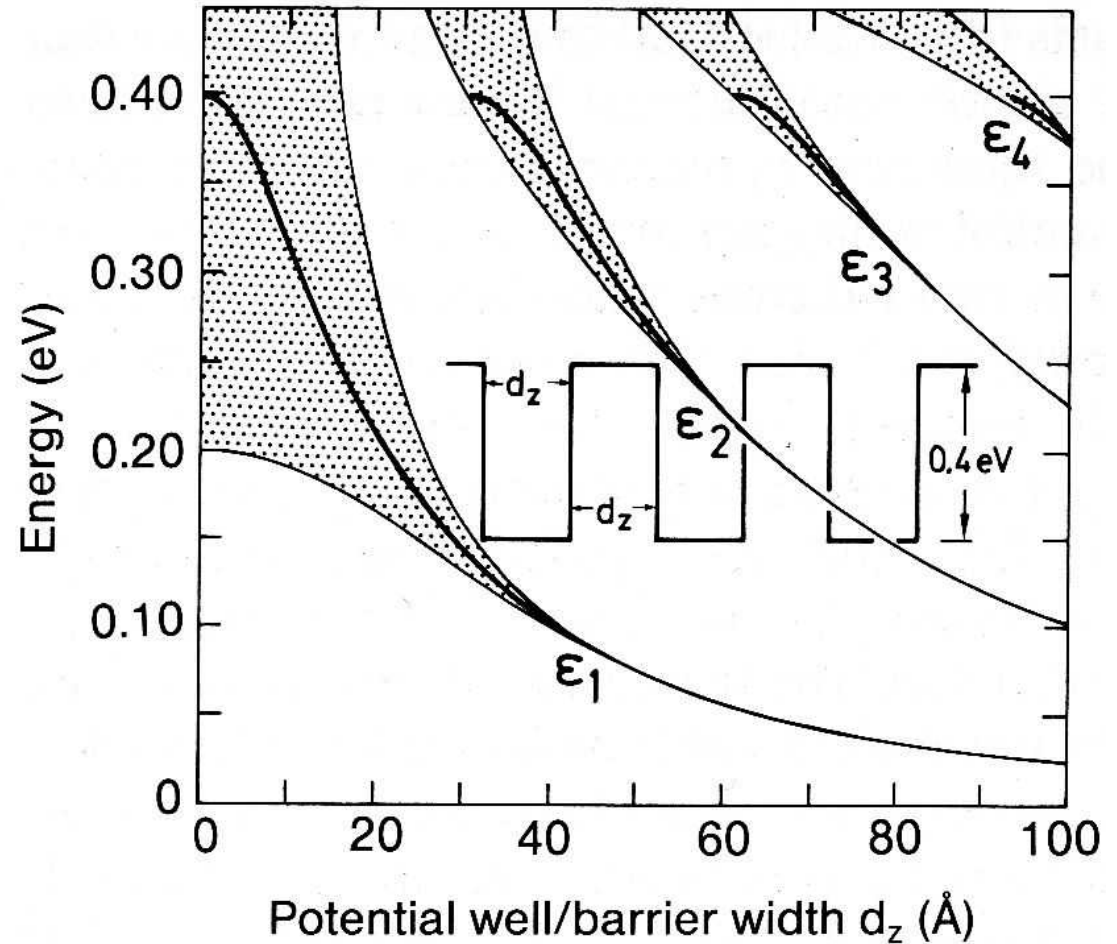
$\mu = 2 \times 10^7 \text{ cm}^2/\text{Vs}$ corresponds to 1/5 mm ballistic electron motion between collisions



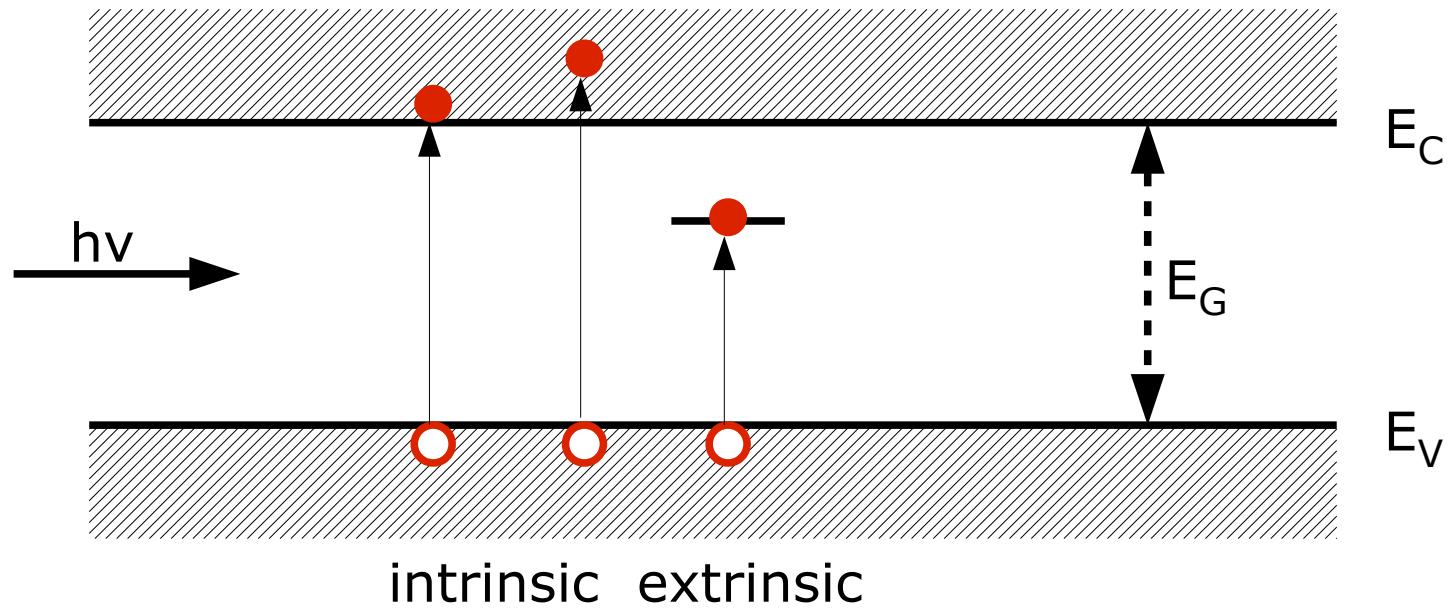
Inventors of the modulation-doping process, in 1978 around an early MBE machine at Bell Labs. From left: Willy Wiegmann, Art Gossard, Horst Störmer, Ray Dingle

Superlattices

Fig. 12.27. Energy states of electrons confined in the rectangular potential wells (inset) of the conduction bands of a composition superlattice; the potential wells have a width d_z which also corresponds to their distance from one another. For the calculation, an electronic effective mass of $m^* = 0.1 m_0$ was assumed. The heavy lines in the shaded regions are the results for single potential wells with the corresponding widths d_z ; potential wells in a superlattice with sufficiently small separation lead to overlap of wavefunctions and therefore to a broadening into bands (shaded region). (After [12.7])



Light Absorption in Semiconductors

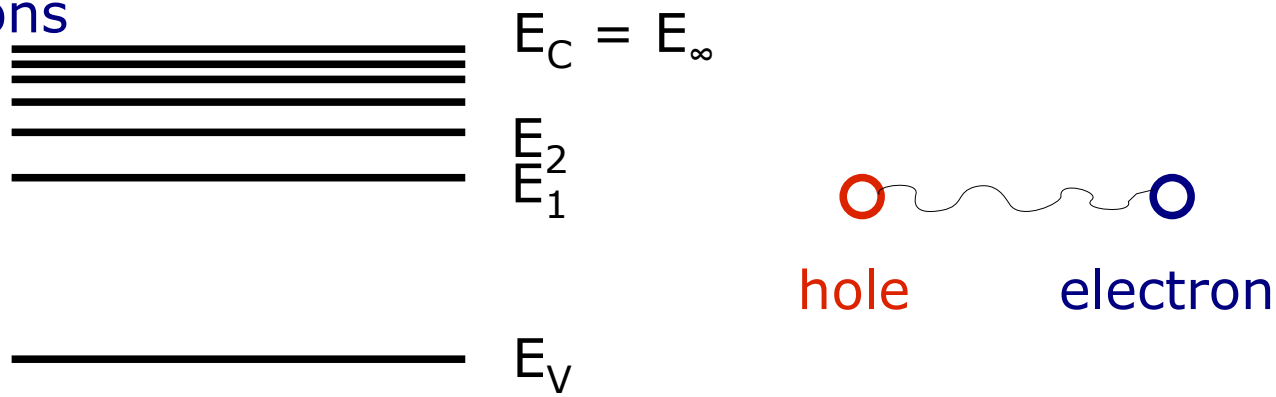


Luminescence

Photoluminescence

Cathodoluminescence; Minority injection, Impact Ionization

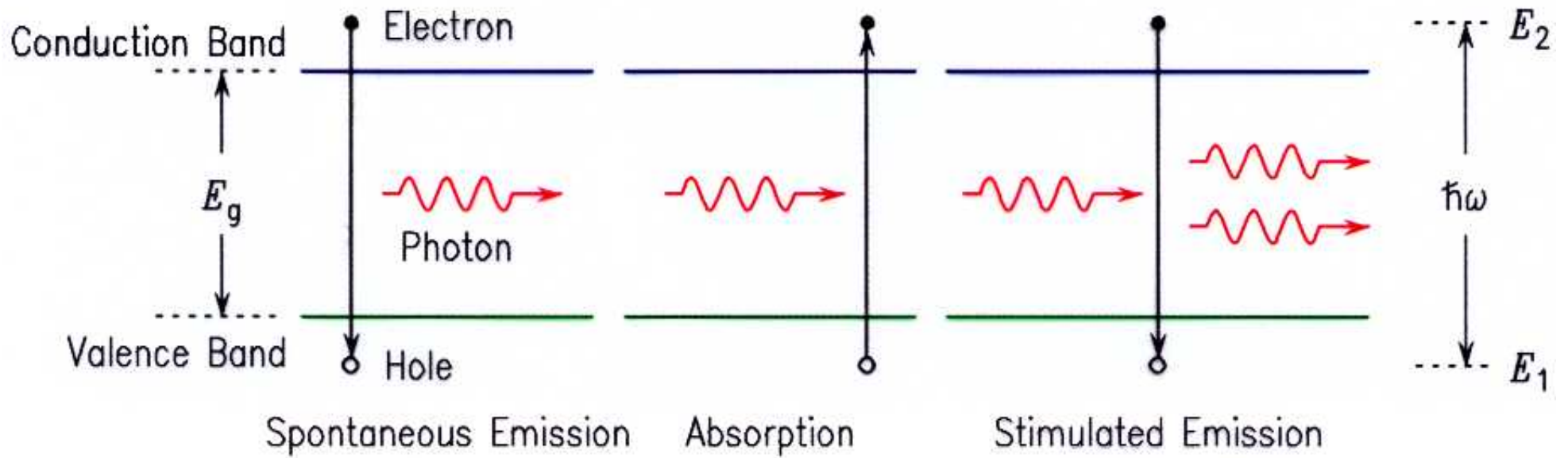
Excitons



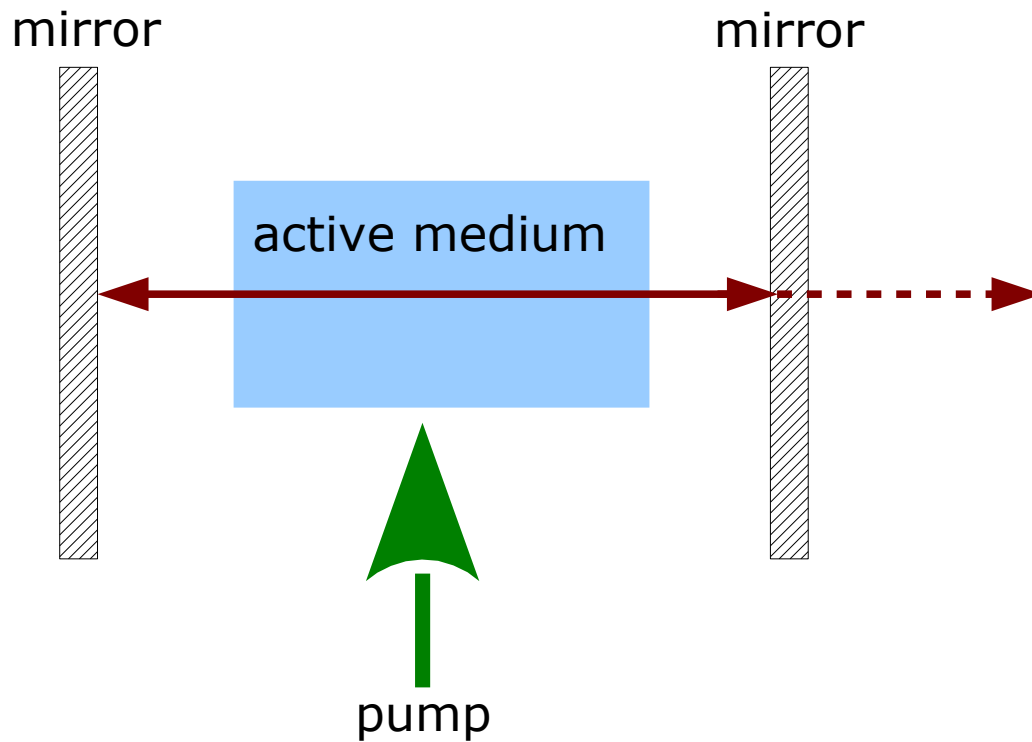
LED – Light Emitting Diode

diode at forward bias – recombination – radiation

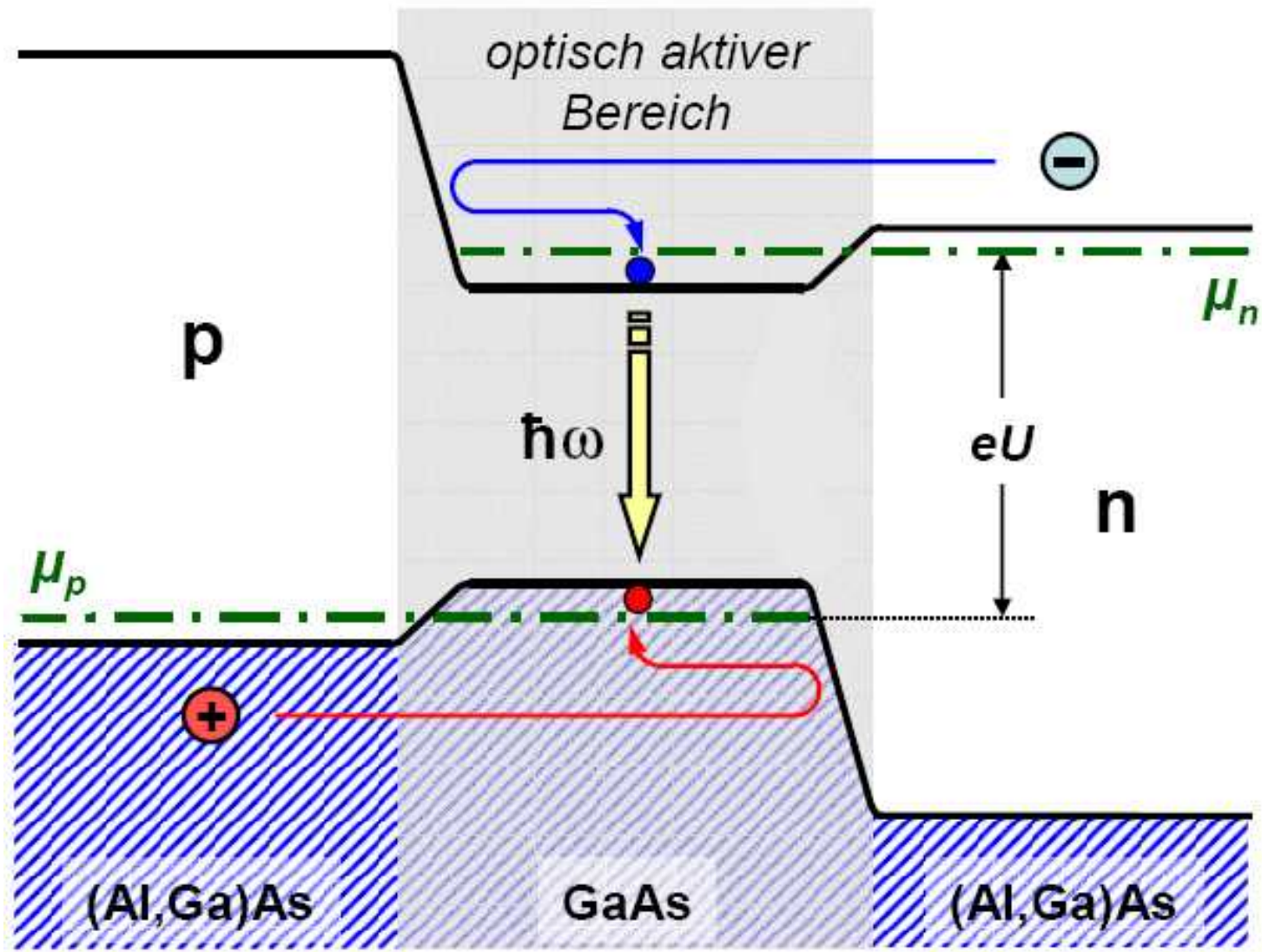
GaAs	1.43 eV	870 nm	IR communication
GaP	2.26 eV	550 nm	green LED
$\text{GaAs}_x\text{P}_{1-x}$	variable		red LED
GaN	3.4 eV	405 nm	violet LED
$\text{In}_x\text{Ga}_{1-x}\text{N}$	variable		blue LED



Laser



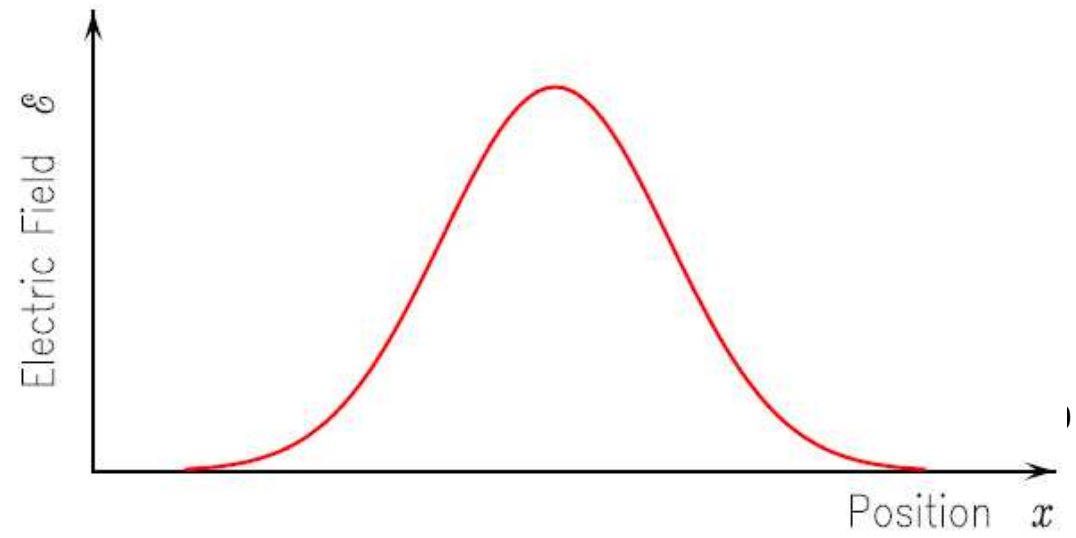
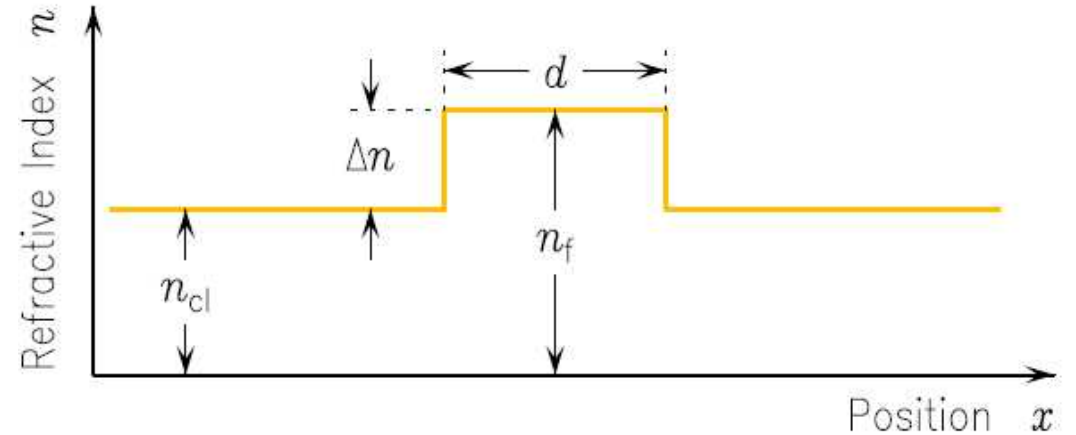
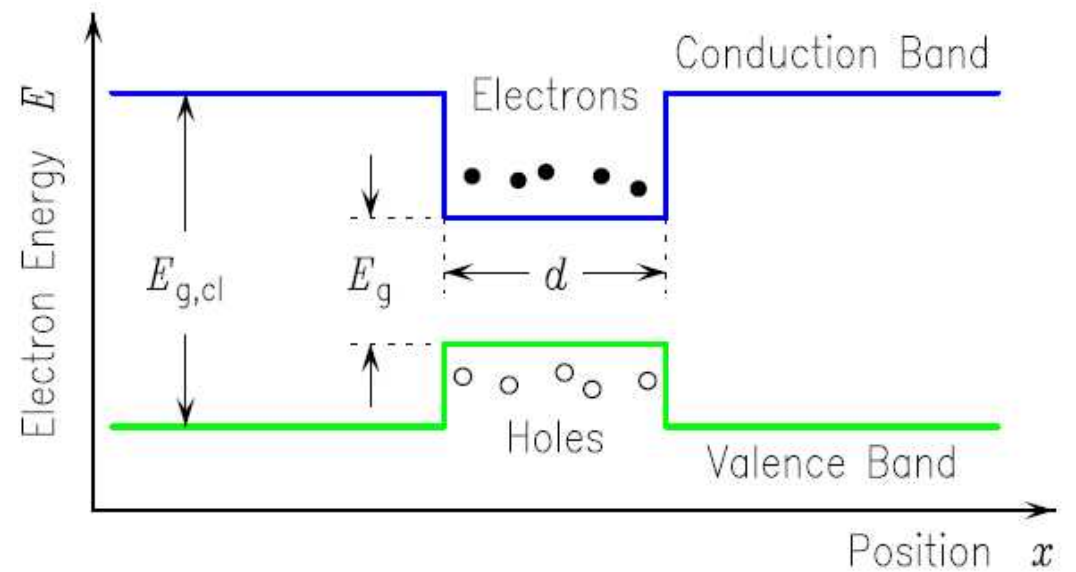
Halbleiterlaser



Halbleiterlaser

Stimulierte Emission:
Maximieren des Lichtfelds
im aktiven Bereich

1. $n(x)$
2. Resonator
(spiegelnde Flächen)



Resonator provides many standing wave modes

$\lambda \approx \text{sub-}\mu\text{m}$ $L \approx \text{mm}$

